

REPORT DOCUMENTATION PAGE

AD-A199 819

2b. DECLASSIFICATION/CONTROLS... ULE		1b. RESTRICTIVE MARKINGS	
4. PERFORMING ORGANIZATION REPORT NUMBER(S)		3. DISTRIBUTION/AVAILABILITY OF REPORT Approved for public release; distribution unlimited.	
6a. NAME OF PERFORMING ORGANIZATION Spire Corp		7a. NAME OF MONITORING ORGANIZATION U. S. Army Research Office	
6b. OFFICE SYMBOL (if applicable)		7b. ADDRESS (City, State, and ZIP Code) P. O. Box 12211 Research Triangle Park, NC 27709-2211	
8a. NAME OF FUNDING/SPONSORING ORGANIZATION U. S. Army Research Office		9. PROCUREMENT INSTRUMENT IDENTIFICATION NUMBER DAAL03-87-C-0027	
8b. OFFICE SYMBOL (if applicable)		10. SOURCE OF FUNDING NUMBERS	
8c. ADDRESS (City, State, and ZIP Code) P. O. Box 12211 Research Triangle Park, NC 27709-2211		PROGRAM ELEMENT NO.	PROJECT NO.
		TASK NO.	WORK UNIT ACCESSION NO.
11. TITLE (Include Security Classification) Deposition of InP on Si Substrates for Monolithic Integration of Advanced Electronics			
12. PERSONAL AUTHOR(S) S. M. Vernon			
13a. TYPE OF REPORT Final	13b. TIME COVERED FROM 9/28/87 TO 3/27/88	14. DATE OF REPORT (Year, Month, Day) May 88	15. PAGE COUNT 25
16. SUPPLEMENTARY NOTATION The view, opinions and/or findings contained in this report are those of the author(s) and should not be construed as an official Department of the Army position, policy, or decision, unless so designated by other documentation.			
17. COSATI CODES		18. SUBJECT TERMS (Continue on reverse if necessary and identify by block number)	
FIELD	GROUP	SUB-GROUP	
19. ABSTRACT (Continue on reverse if necessary and identify by block number)			
20. DISTRIBUTION/AVAILABILITY OF ABSTRACT <input type="checkbox"/> UNCLASSIFIED/UNLIMITED <input type="checkbox"/> SAME AS RPT. <input type="checkbox"/> DTIC USERS		21. ABSTRACT SECURITY CLASSIFICATION Unclassified	
22a. NAME OF RESPONSIBLE INDIVIDUAL		22b. TELEPHONE (Include Area Code)	22c. OFFICE SYMBOL

DTIC
ELECTED
OCT 31 1988
S CD D

FR-10108
May 1988

A Final Report for:
DEPOSITION OF InP ON Si SUBSTRATES FOR MONOLITHIC
INTEGRATION OF ADVANCED ELECTRONICS

Submitted under:
SBIR/Phase I
Contract No. DAAL03-87-C-0027

Submitted to:
U.S. ARMY RESEARCH OFFICE
4300 South Miami Boulevard
Research Triangle Park, NC 27709

Submitted by:
S.M. Vernon, Principal Investigator
SPIRE CORPORATION
Patriots Park
Bedford, MA 01730

SEARCHED	INDEXED
SERIALIZED	FILED
MAY 1988	
FBI - MEMPHIS	
A-1	

TABLE OF CONTENTS

<u>Section</u>	<u>Page</u>
1.0 INTRODUCTION	1
1.1 Background	1
1.1.1 Why InP	1
1.2 InP Substrates	2
1.3 Proposed Approach	2
1.3.1 Benefits of Si	2
1.3.2 Advantages of MOCVD	3
1.4 Literature Review	3
2.0 SUMMARY OF PHASE I RESULTS	5
2.1 Experimental Procedures	5
2.2 Characterization Results	6
2.2.1 Surface Morphology	6
2.2.2 X-ray Diffraction Analysis	12
2.2.3 Double-crystal X-ray Rocking Curve Results	12
2.2.4 Transmission Electron Microscopy (TEM)	17
2.2.5 Electrical Characterization	18
2.2.6 Photoluminescence	18
3.0 SUMMARY	22
4.0 CONCLUSIONS	23
5.0 ACKNOWLEDGEMENTS	23
6.0 REFERENCES	23

LIST OF ILLUSTRATIONS

<u>Figure</u>	<u>Page</u>
2-1	Nomarski Micrographs of InP on (100) Si With Low Temperature InP Nucleation. 7
2-2	Nomarski Micrographs of InP on (100) Si With An In Prelayer. 8
2-3	Nomarski Micrographs of InP on Si by the Single-Step Process as a Function of Substrate Orientation 9
2-4	Nomarski Micrographs of InP-GaAs-Si Samples as a Function of GaAs Layer Thickness 10
2-5	Nomarski Micrographs Comparing Surface Morphologies of InP-GaAs-Si and GaAs-Si Samples 11
2-6	Scanning Electron Micrographs of InP-GaAs-Si Samples 14
2-7	X-Ray Diffractometer Scans of InP on Si With and Without a Thin GaAs Buffer Layer. 15
2-8	Double-Crystal X-Ray Rocking Curve of InP-GaAs-Si Sample #414-3 15
2-9	Double-Crystal X-Ray Rocking Curve of InP-GaAs-Si Sample #405-3 16
2-10	Planview Transmission Electron Micrograph of InP-GaAs-Si Sample #414-2. 19
2-11	Cross-Sectional Transmission Electron Micrograph of InP-GaAs-Si Sample #414-2. 20
2-12	Room-Temperature Photoluminescence of InP-GaAs-Si Sample. 21
2-13	4.4°K Photoluminescence Data for InP-GaAs-Si and InP Homoepitaxial Samples 22

LIST OF TABLES

<u>Table</u>		<u>Page</u>
2-1	InP-on-Si Growth Results	6
2-2	Double-Crystal X-Ray Rocking Curve Data from AT&T Bell Labs.	13
2-3	Double-Crystal X-Ray Rocking Curve Data from SUNY at Buffalo	17
2-4	TEM Results of InP-on-GaAs-on-Si Samples	17
2-5	Room Temperature Photoluminescence Data.	21

1.0 INTRODUCTION

This report describes the results of a Phase I SBIR program entitled "Deposition of InP on Si substrates for Monolithic Integration of Advanced Electronics;" the basic objective of this project was the demonstration of the feasibility of growing high-quality InP layers on Si substrates by the metalorganic chemical vapor deposition (MOCVD) process.

1.1 Background

Recently, the epitaxial growth of III-V compounds on Si has been attracting strong interest. Some reasons for this are that Si is low cost and light weight, has high mechanical strength, excellent crystalline quality and high thermal conductivity and is available as large area substrates. The last and probably most significant reason for growing III-V semiconductors on Si is for monolithic integration of III-V and Si devices, thus combining the high speed and/or optical communication capabilities of III-V's with the sophistication of Si VLSI technology.

Spire is proposing the epitaxial growth of InP on Si substrates for applications as discussed above.

i.1.1 Why InP?

The importance of InP as a semiconductor is based on a number of its material properties. Some of the more important ones are listed below:

- (1) High Peak Velocity of Electrons - The peak (or saturated-drift) velocity of electrons in InP is higher than that of GaAs (2.5×10^7 cm/sec versus 2.2×10^7 cm/sec); this makes InP an excellent choice for transferred-electron devices, such as Gunn diodes, used as very high frequency (millimeter wave) oscillators and amplifiers. Also important is the fact that InP typically has a relatively low noise figure at high frequency.
- (2) Radiation Hardness - This is an important feature for any devices to be utilized in the SDI program. The radiation resistance of InP has been demonstrated (in terms of solar cell experiments) to be quite superior to that of either GaAs or Si.^(1,2) In fact, photovoltaic p/n junction devices irradiated by 1 MeV electrons have been shown to almost totally recover their electrical performance by annealing at room temperature.⁽³⁾

- (2) Low cost - Si substrates are approximately 100 times less expensive than InP;
- (3) Light weight - The density of Si (2.3 gm/cm^3) is about half that of InP (4.7 gm/cm^3);
- (4) Mechanical Strength - Si wafers are much more rugged than InP. An indication of this is the Knoop microhardness values, which are 1150 and 535 kg/mm respectively for Si and InP;
- (5) Thermal Conductivity - The thermal conductivity of Si ($1.68 \text{ W/cm}^\circ\text{K}$) is more than twice that of InP ($0.7 \text{ W/cm}^\circ\text{K}$);
- (6) Monolithic Integration - The epitaxial growth of InP on silicon would allow for the monolithic integration of the optoelectronic and microwave capabilities of InP with the high-speed circuitry of Si VLSI technology.

1.3.2 Advantages of MOCVD

The use of MOCVD is a good choice for the program for the reasons listed below:

- Proven material quality - InP epitaxial layers of excellent electrical quality have been grown by the MOCVD process. Undoped films with 77°K mobilities of $300,000 \text{ cm}^2/\text{V-sec}$ at a background impurity level of $3 \times 10^{13} \text{ cm}^{-3}$ have been achieved.⁽¹¹⁾ Excellent InP/GaInAsP lasers have also been demonstrated with MOCVD-grown layers.⁽⁸⁾
- Volume-amenable process - MOCVD is the technique of choice for the large-scale production of many III-V devices. Reactors up to 1000 cm^2 per batch are currently being used in a production mode for GaAs devices.⁽¹²⁾ Reactor sizes up to 1800 cm^2 per batch have been reported⁽¹³⁾ and much on-going research in terms of material quality and reactor design continue to make MOCVD a rapidly advancing field.

1.4 Literature Review

This section reviews the literature concerning the growth of InP on Si; all these reports utilize the MOCVD technique. In addition, a brief review of the growth of InP on GaAs and GaAs on Si is also presented.

The growth of single crystal InP on Si was first reported in 1986 by researchers at NTT in Japan;⁽¹⁴⁾ since then a few other reports have appeared in the literature.⁽¹⁵⁻²²⁾ The NTT group has succeeded in growing InP films directly on Si substrates and in fabricating solar cells (approximately 3% efficient) from these wafers.⁽¹⁷⁾ These 5- μm -thick InP-on-Si films have been characterized by X-ray rocking curves to have a

2.0 SUMMARY OF PHASE I RESULTS

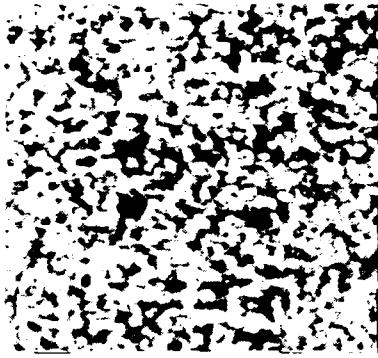
The goal of the Phase I effort was to establish a basic growth process for depositing single-crystal InP films on Si substrates; our experience in growing high-quality GaAs-on-Si and GaP-on-Si structures was to provide a background to guide the experiments.

2.1 Experimental Procedures

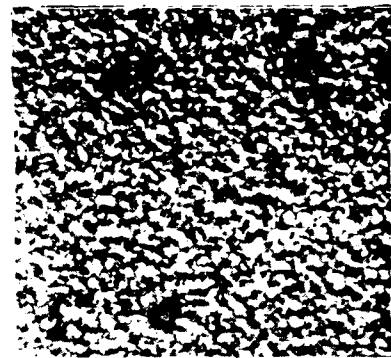
Depositions were carried out by atmospheric-pressure MOCVD in a SPI-MO CVD 450 reactor; the source chemicals used were trimethylindium (TMIn) and phosphine (PH_3) and the main carrier gas was H_2 . The basic GaAs-on-Si growth procedure developed in our laboratory consists of three steps:

1. A high-temperature bakeout in H_2 for 30 minutes at approximately 1000°C
2. A low-temperature nucleation step in which approximately 200 \AA of GaAs is deposited at 400°C
3. A film growth step in which GaAs is grown at "normal" MOCVD conditions utilizing a growth temperature of approximately 675°C

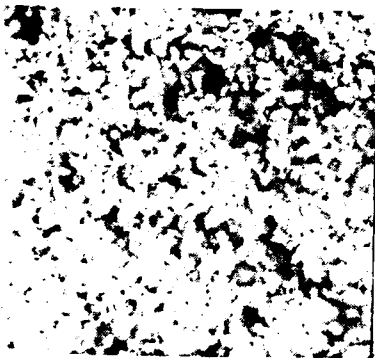
Starting from these basic guidelines, a similar process for InP-on-Si was attempted, with the major variables occurring in Step 2, the nucleation procedure, which is really the most critical step since the surface-oxide-removal procedure (Step 1) had been previously optimized for other heteroepitaxy-on-Si projects. Several different types of nucleation layers/procedures were attempted. These included different materials (InP, In, or P), different thicknesses, and different temperatures; a brief summary of these runs is listed in Table 2-1. In all cases, our standard H_2 bakeout procedure was performed (Step 1), and our standard InP growth conditions (600°C , $1 \mu\text{m/hr}$) were used to grow a thick (1-4 μm) InP layer on top for evaluation. The last two lines of the table are based on conditions used at Spire for deposition-on-Si processes other than the three-step method described above, but which have also shown to be useful. These processes include growing GaAs-on-Si using a nucleation step of pure Ga deposited at the growth temperature of typical GaAs ($\sim 650^\circ\text{C}$), and growing GaP-on-Si by a process which employs a first step of flowing PH_3 over the Si wafer at a temperature of 950°C .



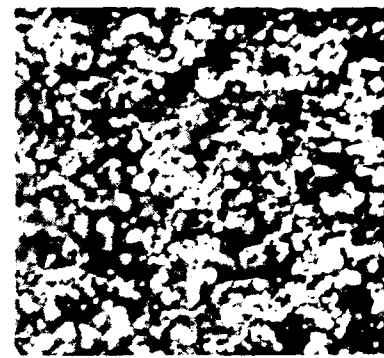
7 SEC



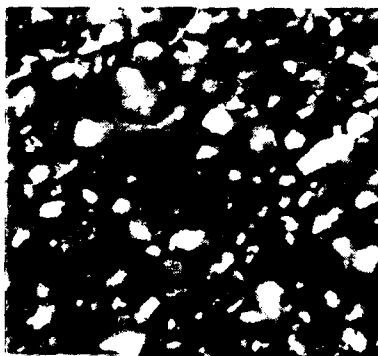
15 SEC



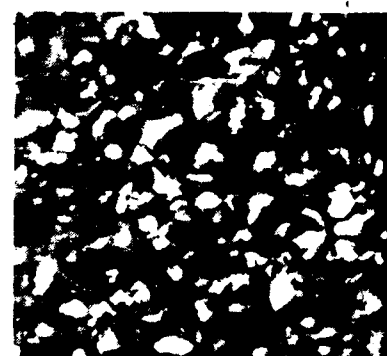
30 SEC



60 SEC



120 SEC



200 SEC

←→
25 MICRONS

FIGURE 2-1. NOMARSKI MICROGRAPHS OF InP ON (100) Si WITH LOW TEMPERATURE InP NUCLEATION. Times shown are for the deposition of the low-temperature layer.

(111)
SILICON
1000X



(100)
SILICON
1000X



←→
25 MICRONS

FIGURE 2-3. NOMARSKI MICROGRAPHS OF InP ON Si BY THE SINGLE-STEP PROCESS AS A FUNCTION OF SUBSTRATE ORIENTATION. The InP growth is at 600°C; the (100) substrate is actually 2° off in the (011) direction.



1000X

**2 μ m InP/Si WITH 1 μ m
GaAs INTERMEDIATE LAYER**



1000X

3 μ m GaAs/Si

←→
25 MICRONS

FIGURE 2-5. NOMARSKI MICROGRAPHS COMPARING SURFACE MORPHOLOGIES OF InP-GaAs-Si AND GaAs-Si SAMPLES. Both samples appear quite specular to the unaided eye.

TABLE 2-2. DOUBLE-CRYSTAL X-RAY ROCKING CURVE DATA FROM AT&T BELL LABS

Sample	Structure	FWHM (arc-sec)	
		InP	GaAs
414-3	4 μ InP-4 μ GaAs-Si	440	320
414-2	4 μ InP-1 μ GaAs-Si	420	470
414-4	4 μ InP-0.1 μ GaAs-Si	400	1000
405-2	1 μ InP-4 μ GaAs-Si	1160	330
405-1	1 μ InP-1 μ GaAs-Si	1380	560
405-3	1 μ InP-0.1 μ GaAs-Si	1420	1770
412-1	1 μ InP-Si	5100	
414-1	4 μ InP-GaAs	260	26
405-4	1 μ InP-InP	11.5	

Data obtained from AT&T Bell Labs, Murray Hill, NJ, through the courtesy of Drs. A. Macrander and S.J. Pearton.

Another point to note in the data of Table 2-2 is that for both the 4 μ m-thick and 1- μ m-thick InP films on GaAs-on-Si, the thickness of the GaAs layer appears to have only a small effect on the quality of the InP layer.

As mentioned above, a few samples were also examined by double-crystal X-ray rocking curve analysis at SUNY at Buffalo by Dr. Wie. These data are shown in Table 2-3. The GaAs-on-Si sample has a small FWHM (180 arc-sec) in this case because it was grown by our more optimized thermal-cycle-growth process⁽³¹⁾ which had not been incorporated into the other samples. The InP-on-GaAs FWHM is larger than that measured at AT&T because the InP layer is thinner; for the InP-GaAs-Si sample, the GaAs FWHM agrees well with the data from AT&T, which was taken on another piece of the same wafer, while there is an unexplained discrepancy in the InP value.

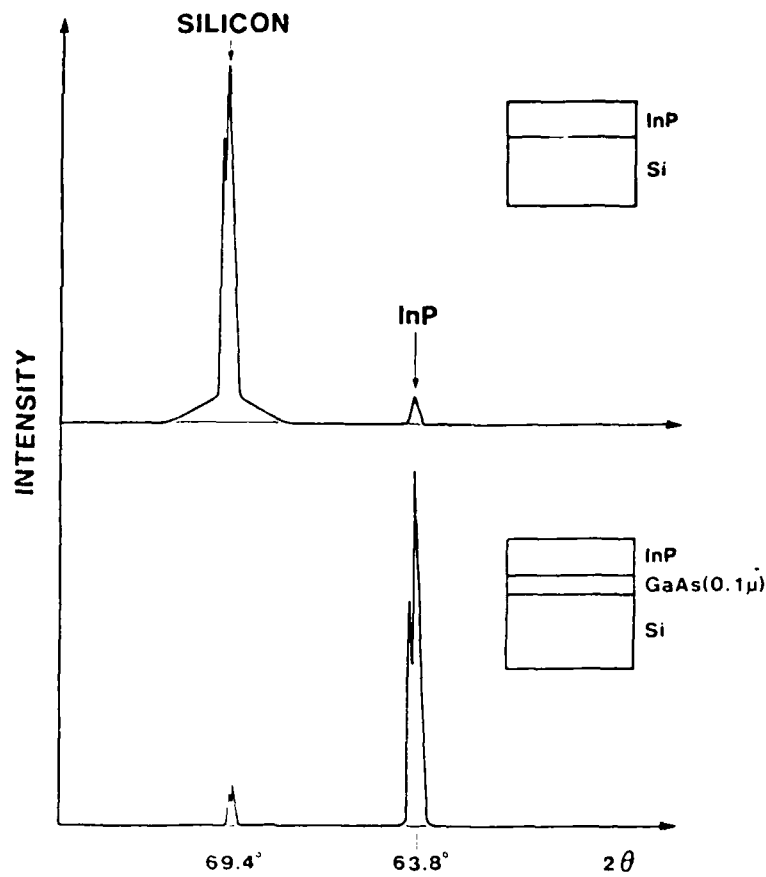


FIGURE 2-7. X-RAY DIFFRACTOMETER SCANS OF InP ON Si WITH AND WITHOUT A THIN GaAs BUFFER LAYER.

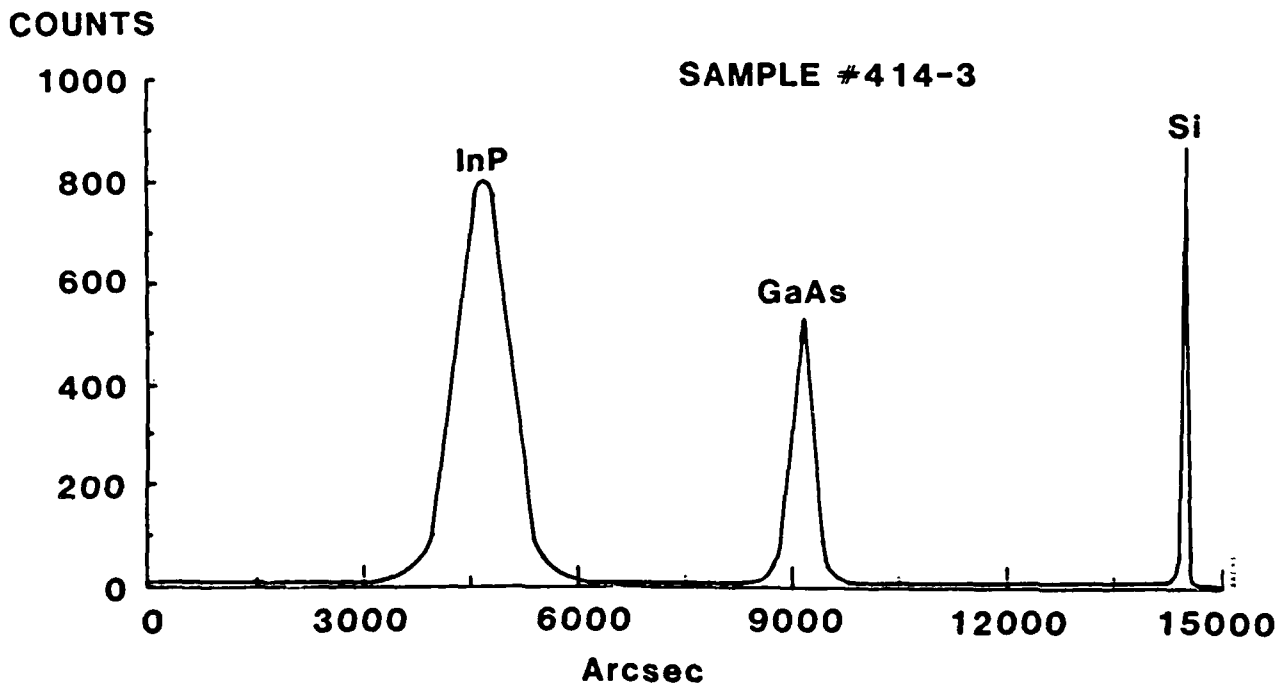


FIGURE 2-8. DOUBLE-CRYSTAL X-RAY ROCKING CURVE OF InP-GaAs-Si SAMPLE #414-3. Data courtesy of AT&T Bell Laboratories.

TABLE 2.3 DOUBLE-CRYSTAL X-RAY ROCKING CURVE DATA FROM SUNY AT BUFFALO

Sample	Structure	FWHM (arc-sec)		Comments
		InP	GaAs	
1326-1	2.3 μ GaAs-Si		180	Thermal Cycle Growth
410-1	2.0 μ InP-GaAs	482		
414-2	4.0 μ InP-1 μ GaAs-Si	576	475	

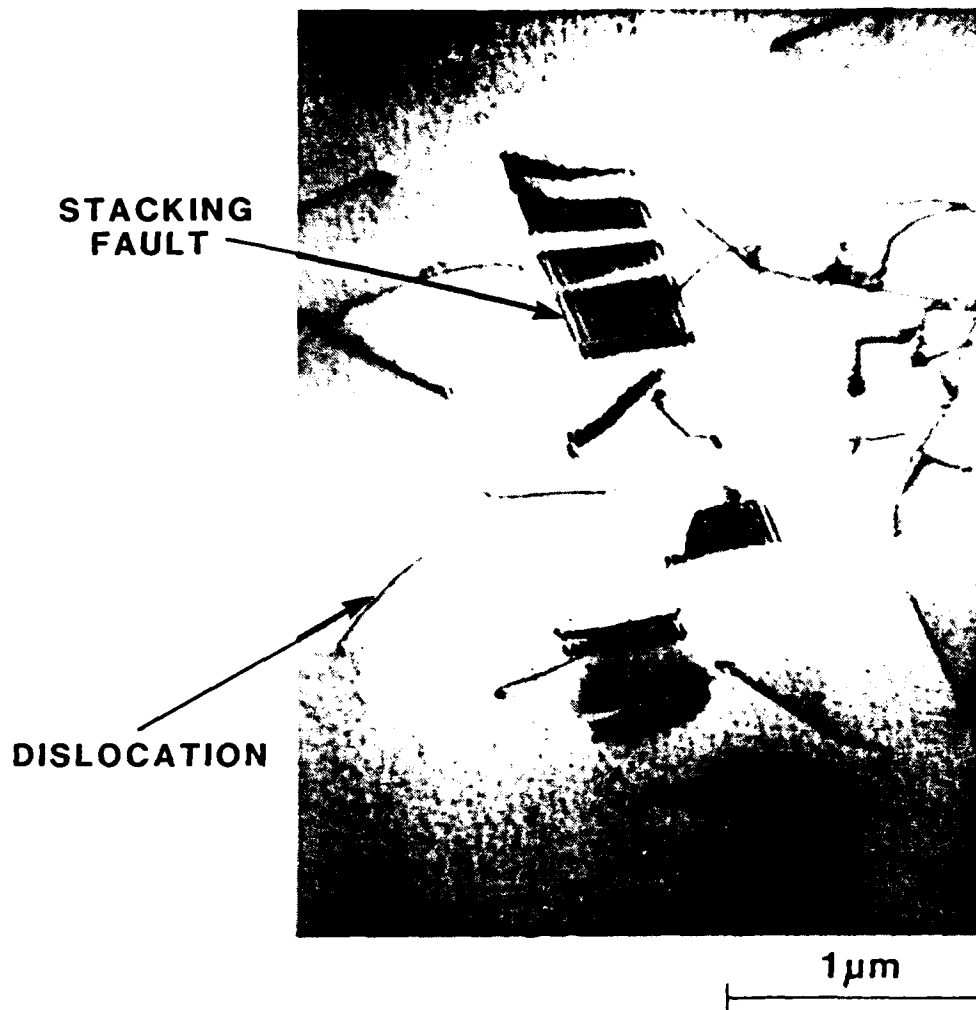
Data obtained from Dr. Chu Wie at SUNY at Buffalo, NY.

2.2.4 Transmission Electron Microscopy (TEM)

Four InP films were analyzed by TEM at the Solar Energy Research Institute (SERI) through the courtesy of Dr. M.M. Al-Jassim. The results are shown in Table 2-4. From these results, we see that a GaAs thickness of 1 μ m appears optimal, and that the defect density of the InP films is identical (within experimental error) to our standard unannealed GaAs-on-Si films ($3 \times 10^8 \text{ cm}^{-2}$). A planview TEM of an InP/GaAs/Si sample is shown in Figure 2-10 where both dislocations and stacking faults are evident. Figure 2-11 shows a cross-sectional TEM of the same sample; it is obvious in this figure that many defects in the InP layer originate at the GaAs-InP interface and are probably not caused by the existing defects in the GaAs layer. This is not surprising, since both interfaces have a lattice mismatch of approximately 4%.

TABLE 2-4. TEM RESULTS OF In-on-GaAs-on-Si SAMPLES

Sample	Thickness (μ m)		Dislocations (cm^{-2})	Stacking Faults (cm^{-2})	Comments
	InP	GaAs			
414-3	4	4	8.4×10^8	1.6×10^8	
414-2	4	1	2.9×10^8	3.6×10^7	
414-4	4	0.1	3.2×10^8	1.0×10^8	
412-1	1	0	-	-	Polycrystalline



InP THICKNESS = 4 μ m, GaAs THICKNESS = 1 μ m

FIGURE 2-10. PLANVIEW TRANSMISSION ELECTRON MICROGRAPH OF InP-GaAs-Si SAMPLE #414-2.

TABLE 2-5. ROOM TEMPERATURE PHOTOLUMINESCENCE DATA

Sample	Structure	FWHM of InP Peak (meV)		Comments
		UCLA	Spire	
414-3	4 μ InP-4 μ GaAs-Si		33.7	Undoped N ~ 10 ¹⁵ cm ³
414-2	4 μ InP-1 μ GaAs-Si	34.4	33.7	Undoped N ~ 10 ¹⁵ cm ³
414-4	4 μ InP-0.1 μ GaAs-Si		30.8	Undoped N ~ 10 ¹⁵ cm ³
405-2	1 μ InP-4 μ GaAs-Si		69.9	Doped N ~ 10 ¹⁷ cm ³
405-1	1 μ InP-1 μ GaAs-Si	59.7	66.8	Doped N ~ 10 ¹⁷ cm ³
405-3	1 μ InP-0.1 μ GaAs-Si		66.8	Doped N ~ 10 ¹⁷ cm ³
405-4	1 μ InP-InP	59.7	77.8	Doped N ~ 10 ¹⁷ cm ³

4 μ InP / 1 μ GaAs / Si 300°K

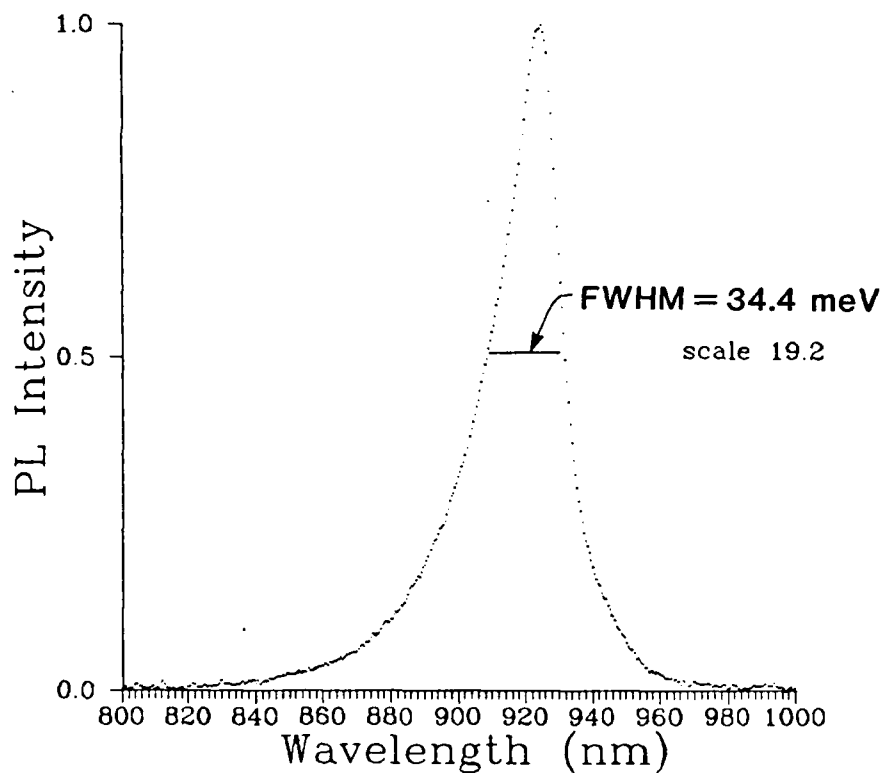


FIGURE 2-12. ROOM-TEMPERATURE PHOTOLUMINESCENCE OF InP-GaAs-Si SAMPLE. Data courtesy of UCLA.

- The InP-GaAs interface appears to generate as many dislocations as does the GaAs-Si interface.
- InP-GaAs-Si samples show reasonably good PL at room-temperature and 4.4°K and that the PL halfwidth at 300°K is fairly insensitive to the GaAs buffer thickness.

4.0 CONCLUSIONS

The Phase I effort has led us to make the following conclusions:

- The feasibility of deposition single-crystal InP-on-Si structures by MOCVD has been clearly demonstrated in this program.
- The use of a thin GaAs buffer layer facilitates the growth of high-quality, single-crystal InP overlayers on Si substrates.
- Much optimization of the heteroepitaxial structure and growth process is possible.

5.0 ACKNOWLEDGEMENTS

The principal investigator wishes to acknowledge the contributions of the following people:

- Dr. M.M. Al-Jassim for TEM studies at SERI.
- Drs. S.J. Pearton and A. Macrander for X-ray analyses at AT&T Bell Laboratories.
- Drs. N.M. Haegel and V.P. Mazzi for PL characterization at UCLA.
- Mr. V.E. Haven for MOCVD growth at Spire.

6.0 REFERENCES

1. A. Yamamoto, M. Yamaguchi, and C. Uemura, Appl. Phys. Letters, 44, 611 (1984).
2. M. Yamaguchi, C. Uemura, and A. Yamamoto, J. Appl. Phys. 55, 1429 (1984).
3. M. Yamaguchi, Y. Itoh, and K. Ando, Appl. Phys. Letters, 45, 1206 (1984).
4. M. Ogura, K. Inove, and Y. Ban, Japan J. Appl. Phys. 21, L598 (1982).
5. G. Post and A. Mircea, Electron Letters, 19, 460 (1983).
6. H. Damokes, V. Konig, and B. Schwaderer, Electron Letters, 20, 957 (1984).

27. For a good review see Heteroepitaxy on Si, Mater. Res. Soc. Symp. Proc. 67 (1986), and Heteroepitaxy on Si II, Mater. Res. Soc. Symp. Proc. 91 (1987).
28. H. Morkoc, Mater. Res. Soc. Symp. Proc. 67, 149 (1986).
29. D.G. Deppe, N. Holonyak, D.W. Nam, K.C. Hsieh, G.S. Jackson, R.J. Matyi, H. Shichijo, J.E. Epler, and H.F. Chung, Appl. Phys. Lett. 51, 637 (1987).
30. S.J. Pearton, C.R. Abernathy, R. Caruso, S.M. Vernon, K.T. Short, J.M. Brown, S.N.G. Chu, M. Stavola, and V.E. Haven, J. Appl. Phys. 63, 775 (1988).
31. M.M. Al-Jassim, R.K. Ahrenkiel, D.J. Dunlavy, K.M. Jones, S.M. Vernon, S.P. Tobin, and V.E. Haven, Appl. Phys. Lett., 1988 (to be published).
32. S.J. Pearton, D.L. Malm, L.A. Heinbrook, C.R. Abernathy, R. Caruso, S.M. Vernon, and V.E. Haven, Appl. Phys. Lett. 51, 682 (1987).